Desalination and Water Treatment
www.deswater.com

doi: 10.1080/19443994.2015.1091993

57 (2016) 17075–17086
August

Taylor & Francis
Taylor & Francis Group

Study of salinity variation in the Sebou River Estuary (Morocco)

S. Haddout[a,*], A. Maslouhi[a], B. Magrane[b], M. Igouzal[a,*]

[a]*Interdisciplinary Laboratory for Natural Resources and Environment, Faculty of Sciences, Department of Physics, Ibn Tofail University, B.P 242, 14000 Kenitra, Morocco, emails: haddout.ens@gmail.com (S. Haddout), maslouhi_a@yahoo.com (A. Maslouhi), igouzal@univ-ibntofail.ac.ma (M. Igouzal)*
[b]*Ministry of Energy, Mines, Water and Environment, Water Service of Kenitra City, B.P 203, 14000 Kenitra, Morocco, email: magraneb@yahoo.fr*

Received 5 March 2015; Accepted 26 August 2015

ABSTRACT

The Sebou river estuary is a coastal zone with an important agricultural area and is becoming one of the most important industrial zones in Morocco. However, salt water intrusion affects the economic development of the whole region. Therefore, determination of the salinity distribution along this estuary is the main interest for water managers. The aim of this paper is to study the spatial and temporal distribution of salinity in water course. Field measurements revealed that salinity intrusion depends on the state of the tide and on the upstream tributary waters from Lalla Aïcha Dam. The effects of the combination of various situations (dam closed–dam open and high tide–low tide) have been studied. A one-dimensional mathematical model has been used to simulate salinity distribution along the estuary. The model is based on one-dimensional equations of continuity, momentum, and salt transport in natural waters. Calculations of the river water level provided by the model are in good agreement with field measurements. Additionally, salinity simulations along the Sebou estuary for different hydrodynamic river conditions reproduce the observed salinity trends and contribute to a better understanding of this natural phenomenon. The model used permits a rapid assessment of salt water intrusion in the Sebou estuary and can help to ensure the safety of water supply and to support decision-making interventions.

Keywords: Sebou river estuary; Salinity intrusion; Mathematical model; HEC-RAS

1. Introduction

Water resources are necessary for the development of human societies. This development, mainly in the industrial and agricultural sectors, increasingly affects these resources at many levels. Lack of water is considered as a limiting factor of socio-economic development of a country. A major objective is to establish policies for sustainable management and governance rules of water resources so as to ensure their durability [1].

Regarding Morocco, conventional water resources are very limited and irregular. This is due to the increase in several activities (e.g. intensive agriculture,

*Corresponding authors.

Presented at the 7th International Conference on Water Resources in the Mediterranean Basin (WATMED7) 8–11 October 2014, Marrakesh, Morocco

and various industries) using water and also to the influence of climate change. This situation urges us to look for other water resources not yet exploited (e.g. water available in estuaries).

An estuary is a semi-enclosed coastal body of water, which has a free connection with the open sea and within which sea water is gradually diluted with fresh water derived from land drainage [2,3]. Salt water intrusion is one of the most important physical phenomena in estuaries that affects the quality of both surface and ground water [4].

The Sebou is the largest Moroccan river, draining approximately 40.000 km^2, stretching about 614 km from its source in the middle Atlas mountains to the Atlantic Ocean, which represents 6‰ of Morocco's total land area (Fig. 1). Kenitra harbor, about 17 km from the ocean, has commercial traffic, while Mehdia harbor at only 2 km from the mouth is busy with fishing activities.

The flow regime at the level of the Sebou estuary is marked by considerable seasonal and inter-annual variations. It is under the influence of the tide regime and under the control of many dams [5,6]. During low flow periods, hydrodynamic regime is controlled by the Lalla Aïcha dam situated 62 km upstream. This dam has been constructed to preserve water for agricultural pumping stations and to avoid salty waters that rise towards these stations. Before the dam construction, excessive salinity reached up to 85 km upstream [7].

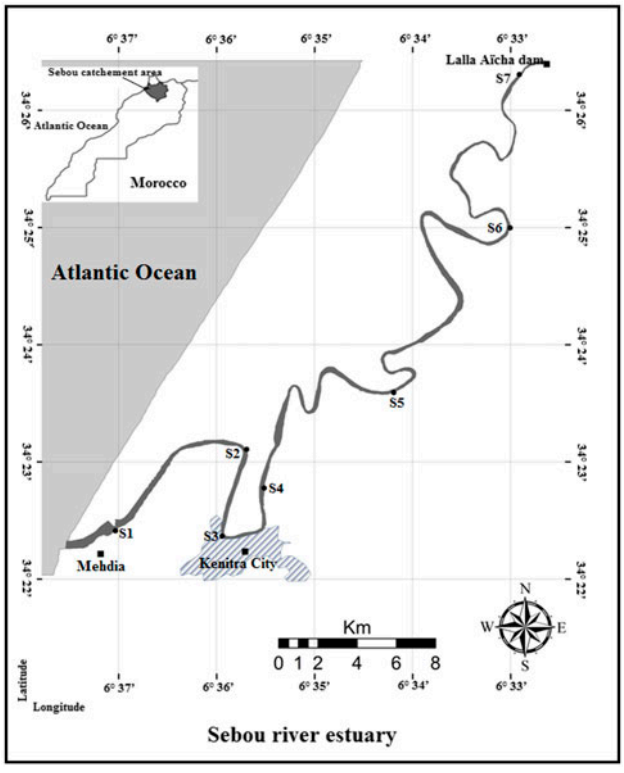

Fig. 1. Study area and measurements sites in the Sebou river estuary.

Salinity concentration of the estuary varies between 0.5 and 35‰. The tide regime in the estuary is characterized by a filling at high tide by the bottom of the river and by a emptying at low tide [8]. The semi-diurnal tidal range varies from 0.97 to 3.11 meters and tidal influence extends 35 km from the mouth [9]. In addition, the Sebou estuary is considered as a narrow estuary, so wind has minimum impact on the flow [10].

The waters in the Sebou river estuary are used by many industries and for agriculture supply. However, high water salinity limits the development of these activities.

Early works on salinity distribution in Sebou river estuary has started since 1966 [7]. All these works were based on field measurements and did not examine salinity evolution influence toward hydrodynamic and morphological conditions. In a management context, rapid estimation of longitudinal salinity distribution in an alluvial estuarine is searched by managers. One-dimensional mathematical models can constitute the appropriate tools to use because they are easy to apply, and more adapted to management contexts. Also, it is methodologically correct to start with the simplest description of the phenomena under study and to evaluate the limits of this approximation before investigating more complications.

In this paper we have studied the spatial and temporal evolution of longitudinal salinity distribution in the Sebou river estuary. Field measurements were realized in a wide range of situations of the tide and the dam situations. The influence of the total closure of the dam on the salt concentration has been evaluated for the first time. The one-dimensional mathematical model HEC-RAS [11] has been used to simulate salt water intrusion. Firstly, simulation of the hydrodynamic regime of the river has been undertaken. Substantial database was used, consisting of river morphology, friction factors, river flows, and river water levels. These data were used to calibrate the hydrodynamic model, which was later linked to the transport model. The outputs of the transport model are the salt evolution from upstream to downstream of the estuary for various hydrodynamic conditions. The model allows estimating salinity variation even at zones where we do not dispose of field data. It also permits to draw isohaline charts (areas of equal salinity) for different situations.

2. Stations and measurement methods

The studied reach (62 km) is situated between the mouth of Sebou river and Lalla Aïcha dam (Fig. 1). Salinity measurements were made at specific stations in order to consider their spatial variability (see Table 1). As some stations correspond to stations used in other works [7,8,12] we have been able to compare results obtained from each study. For the salinity measurements, a Water Meter Type 120-LTC Conductivity Meter attached with 120 m cable was employed. This instrument is able to measure water temperature and salinity simultaneously. It is worth to note that the conductivity and temperature have to be calibrated before use. Also, Global Positioning System (GPS) was used to record the locations of every measurement.

3. Results and discussion

3.1. Field measurements

In order to study the temporal variability of the salinity, 24 h field measurements (06–07 Jun 2014) were conducted at the S3 station, with 10-min interval. Fig. 2 shows a sinusoidal salinity evolution, which follows the tidal cycles. A maximum concentration of 30‰ is recorded during high tides and a minimum concentration of 5‰ is recorded during low tides.

The hydrodynamic regime of the Sebou estuary is influenced by the tidal cycle (at the mouth of the river) and water flow releases from the Lalla Aïcha dam. The influence of the hydrodynamic regime on salinity evolution along the estuary was studied by making salt measurements for various situations of the tide and the river flow (Fig. 3). Fig. 4 presents similar measurements made by the ministry of energy between 2004 and 2012. The two figures show that a descending salinity gradient (downstream–upstream) is observed in all the situations, caused by the gradual salinity intrusion from the sea.

Table 1
Locations of measurement stations

Station	Distance at the mouth
Station 1	(Mouth of the river)
Station 2	12 km
Station 3	17 km (Kenitra City)
Station 4	34 km
Station 5	40 km
Station 6	53 km
Station 7	62 km (Lalla Aïcha Dam)

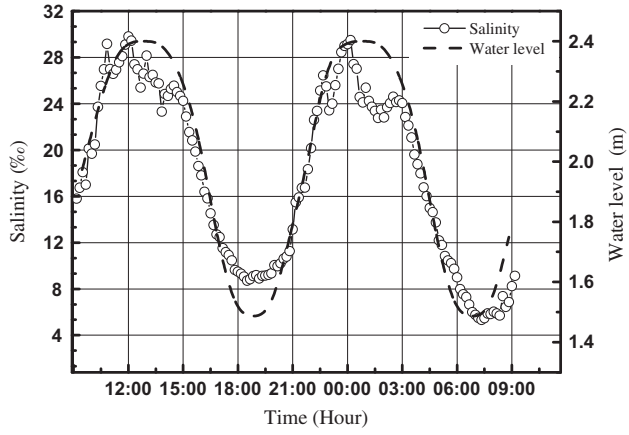

Fig. 2. Salinity evolution at the S3 station: During 24 h (06–07 June 2014).

Salinity concentration varies between 12 and 35‰ at the mouth of the river and does not exceed 0.8‰ at 40 km at the downstream part of the river. In addition, figures also show an increase in salt concentration during high tide along the reach, highlighting the effect of the salinity intrusion. Fig. 4 shows the effect of a total closure of Lalla Aïcha dam on salt evolution along the studied reach. When no fresh water is spilled downstream the dam, salt concentration rises to high levels along the river. This phenomenon is highlighted for the first time and imposes the need to consider the dam management in excessive salt progression studies.

All measurements shown above enabled us to divide the river, according to the salinity categories (zones) of the Venice System [13] (Table 2), from limnetic (salinity 0.5‰) to fully marine waters (30‰).

The limnetic zone is situated between stations S6 and S7 (9 km) where salinity does not exceed 2‰, and is not influenced by tidal dynamics. The mesohaline/oligohaline zone is situated between stations S3 and S6 (36 km), where the salinity is between 2 and 12‰. This zone is considered a transition zone influenced by tidal dynamics and river flow. The polyhaline/euhaline zone is situated between stations S1 and S3 (17 km), where the oceanic influence is permanent, regardless of the river flow downstream Lalla Aïcha dam. The salinity in this area is between 12 and 34‰. All zones position see Fig 5.

On other hand, we examine the vertical salinity and temperature measurements of the Sebou river estuary. A notable stratification is observed, essentially for stations near the estuary mouth (S1, S2, S3, and S4). Fig. 6 gives an example of this stratification in the S3 station where salinity and temperature gradient between the surface and the bottom of the river, are

Table 2
Classification of estuarine divisions (expanded from McLusky, 1993) (salinity is defined according to the Practical Salinity Scale) [13]

Division	Tidal	Salinity (‰)	Venice system (1958)
River	Non-tidal	<0.5	Limnetic
Tidal fresh	Tidal	<0.5	Limnetic
Upper	Tidal	0.5–5	Oligohaline
Inner/Middle	Tidal	5–18	Mesohaline
Middle/Lower	Tidal	18–30	Polyhaline
Mouth	Tidal	>30	Euhaline

6‰ and 0.5°C, respectively. Sea waters have a high density and low temperature compared to fresh waters and tends to dive to the bottom of the river. This result confirms that the filling and emptying of the Sebou river estuary is achieved from the bottom as mentioned above [8].

The salt water intrusion is generally divided into three types according to the level of stratification [14,15]: Salt-wedge estuary, well-mixed and partially mixed estuary. A salt-wedge estuary occurs when the freshwater discharge in an estuary is large compared to the tidal flows. In a partially mixed estuary, the river has a strong surface flow of freshwater and a strong influx of seawater. Tidal currents force the seawater upward, where it mixes with the surface water, producing a seaward flow of surface water. The salinity is increased by the influx of seawater. In well-mixed estuary, the river flow is low, and tidal currents play a major role in water circulation. The net result is a seaward flow of water and uniform salinity at all depths. This classification involves the so-called estuary number, N_e, whose values, given by (Eq. (1)) [16] are listed in Table 3.

$$N_e = \frac{V_{EO}.U_0^2}{g.d.Q_f.T} \quad (1)$$

where V_{EO} is the volume entering the mouth of the estuary during the rising tide (m^3), Q_f is the river flow ($m^3 s^{-1}$), U_0 is the maximum velocity at the river mouth ($m s^{-1}$), d is the depth at the mouth of the estuary (m), T is the tidal period (s), and g is the acceleration due to gravity ($m s^{-2}$).

In the case of Sebou estuary, for a river flow of 10 $m^3 s^{-1}$, which corresponds to the flow during the measurement in Fig. 6, the calculated value of the estuary number is 0.32. According to the classification above, this value of N_e corresponds to a partially mixed estuary, which is consistent with observations at the same figure. For a flow of 40 $m^3 s^{-1}$, the calculated value of N_e is 0.064 corresponding to a salt-wedge river. Thus, the levels of stratification in the Sebou river estuary depend strongly on the river flow.

3.2. Mathematical modeling

To model the salinity evolution along the Sebou estuary, we used a one-dimensional approach which is appropriate in the case of the river reach having long distance. The HEC-RAS mathematical model was used in this study. It was used to simulate the hydrodynamic regime, sediment transport, and water quality for many rivers [11]. Salinity distribution is influenced by the hydrodynamic regime of the Sebou river estuary, which in turn depends highly on the river morphology. For this reason, the hydrodynamic regime was first studied and modeled in the HEC-RAS. Outputs from the hydrodynamic model (velocity and water level evolution) were used in the salt transport study.

3.2.1. Hydrodynamic model

In the present study, unsteady, gradually varied flow simulation model, i.e. HEC-RAS, is based on the Saint-Venant's two equations commonly used in river hydrodynamics, which are defined as follows [11]:

Table 3
Classification of estuaries according to the value of the number of estuary N_e

N_e	Ne < 0.08	0.08 < Ne < 0.5	Ne > 0.5
Classification	Salt-wedge estuary	Partially-mixed estuary	Well-mixed estuary

$$\frac{\partial Q}{\partial x} + \frac{\partial A}{\partial t} = q_l \tag{2}$$

$$\frac{\partial Q}{\partial t} + \frac{\partial (Q^2/A)}{\partial x} + g.A.\frac{\partial h}{\partial x} - g.A.(S_f - S_0) = 0 \tag{3}$$

where Q is the discharge ($m^3\ s^{-1}$), A is the cross-sectional area (m^2), x is the distance along the channel (m), t is the time (s), q_l is the lateral inflow per unit length ($m^2\ s^{-1}$), g is the acceleration due to gravity ($m\ s^{-2}$), h is the flow depth (m), S_0 is the bottom slope (Dimensionless), and S_f is the frictional slope (Dimensionless).

The frictional slope is expressed as [6]:

$$S_f = \left[\frac{n\,Q}{A\,R^{2/3}}\right]^2 \tag{4}$$

where n is Manning's roughness coefficient ($m^{-1/3}\ s^{-1}$), and R is the hydrodynamic radius (m).

The Manning coefficient used in the momentum equation is evaluated initially by the empirical formula (Eq. (5)) proposed by Cowan and Chow [17,18].

$$n = (n_0 + n_1 + n_2 + n_3 + n_4).m_5 \tag{5}$$

where n_0 is a basic, n is the value for a straight, uniform, and smooth channel, n_1 is the adjustment for the effect of surface irregularity, n_2 is the adjustment for the effect of variation in shape and size of the channel cross section, n_3 is the adjustment for obstruction, n_4 is the adjustment for vegetation, and m_5 is a correction factor for meandering channels.

The factor n_0 is evaluated from granulometric measurements that were carried out from upstream to downstream in the studied reach. The others coefficients were evaluated from observations of the river in aerial photos, from the cross-sectional areas and available photos, and from field visits.

The Eqs. (2) and (3) are solved using the well-known four-point implicit box finite difference scheme. The general implicit finite difference forms for a function f are [11]:

The Time derivative:

$$\frac{\partial f}{\partial t} \approx \frac{\Delta f}{\Delta t} = \frac{0.6\,(\Delta f_{j+1} + \Delta f_j)}{\Delta t} \tag{6}$$

The Spatial derivatives:

$$\frac{\partial f}{\partial x} \approx \frac{\Delta f}{\Delta x} = \frac{(f_{j+1} - f_j) + \theta\,(\Delta f_{j+1} + \Delta f_j)}{\Delta x} \tag{7}$$

Function value:

$$f \approx \overline{f} = 0.6\ (f_j + f_{j+1}) + 0.6.\,\theta.(\Delta f_{j+1} + \Delta f_j) \tag{8}$$

where θ: weighting factor.

This numerical scheme has been shown to be completely non-dissipative but marginally stable when run in a semi-implicit form, which corresponds to weighting factor (θ) of 0.5 for the unsteady solution. This value represents a half weighting explicit to the previous time step's known solution, and a half weighting implicit to the current time step's unknown solution. However, practically speaking, due to its marginal stability for the semi-implicit formulation, a θ weighting factor of 0.6 or more is necessary, since the scheme is diffusive only at values of θ greater than 0.5. In HEC-RAS, the default value of θ is 1. However, the user can specify any value between 0.6 and 1 [19].

The final resolution of model equations requires spatial discretization of the study area. The river reach (62 km) was discretized into 203 grids with a length varying between 58 and 996 m. Data on cross sectional (bathymetry) areas from the ANP (National Agency of Ports) and other sources were used.

The upstream boundary (at the Lalla Aïcha dam) was given values of discharge as a function of time (Fig. 7). The downstream boundary (at the mouth) was given values of the water level as a function of time (Fig. 8).

3.2.1.1. Model calibration and validation. The Hydrodynamic model has been calibrated and validated. The calibration parameter is Manning's roughness in the river. Initial values of Manning's roughness vary along the studied reach, with a mean value of $0.051\ m^{-1/3}\ s^{-1}$. In the calibration procedure, the Manning coefficient was modified to the same degree along the studied reach because we assumed that the sources of errors involved in its evaluation are identical for all the grids.

The calibration and validation are performed using the water level data at the S3 station. The period chosen for the calibration was from 01 May 2014 to 15 May 2014. Fig. 9 gives the results of the calibration. This figure shows good correspondence between the calculated and the observed water level at the S3 station.

In order to confirm the results of the calibration test, we proceeded with a validation test of the model for the period from 15 May 2014 to 30 May 2014. Fig. 10 shows the comparison of observed and simulated water level at the S3 station.

In addition, a model performance has been tested by statistical indicators: the root-mean squared error (RMSE), the Nash–Sutcliffe modeling efficiency index (NSC), and the correlation coefficient (R^2). The equations used to determine these indicators are available in [20–22].

The RMSE indicates a perfect match between observed and predicted values when it equals 0. The NSC ranges between $-\infty$ and 1. It indicates a perfect match between observed and predicted values when it is equal to1. Values between 0 and 1 are generally viewed as acceptable levels of performance [22].

Table 4 gives the values obtained for each of these indicators for calibration and validation results.

The RMSE, Nash–Sutcliffe efficiency coefficient (NSC), and the R^2, all show that the model has a good performance in water level prediction.

3.2.1.2. Hydrodynamics results. After the calibration and the validation, the model outputs are more reliable; they give more detailed information about the hydrodynamic regime of the river.

Fig. 11 shows calculated velocity at low tide and high tide along the studied reach. Great variations of velocity can be seen due to the changes in the river geometry. Also, the velocity is strongly influenced by tidal conditions. Fig. 12 shows simulation of water level at the S6 station during May 2014. Water level is influenced by tidal conditions and also by upstream inflows of the river.

Table 4
Statistical indicators of the hydrodynamic model performance

Statistical indicators	RMSE (m)	NSC	R^2
Calibration	0.08	0.92	0.89
Validation	0.10	0.95	0.90

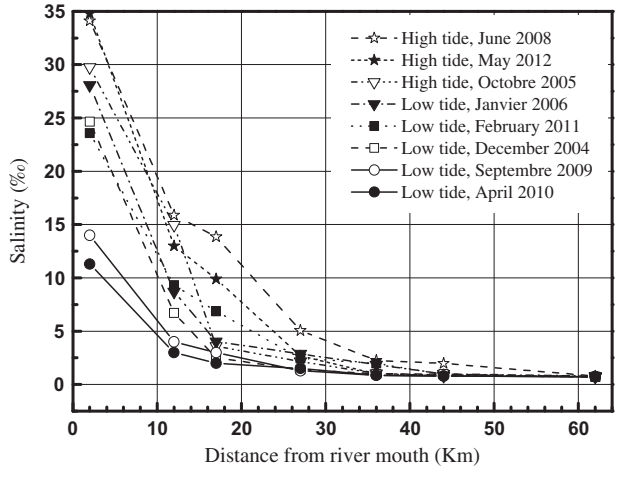

Fig. 3. Longitudinal salinity distribution between 2004 and 2012 (Ministry of Energy).

3.2.2. Transport model

Water quality modeling is often applied as a supporting tool for water quality management [23]. Modeling salinity evolution was achieved using Water Quality module included in HEC-RAS software. It is

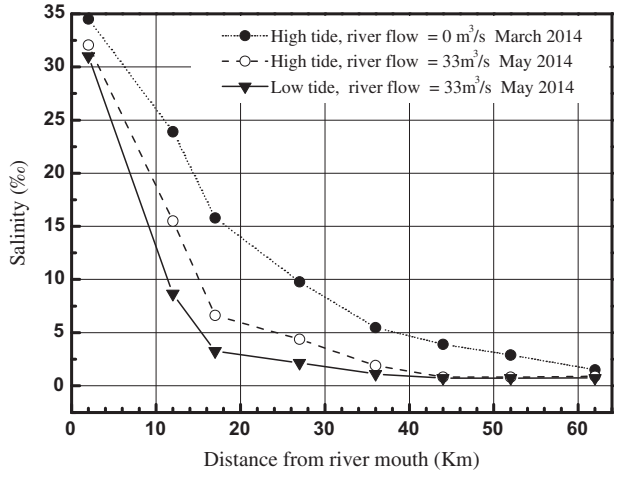

Fig. 4. Longitudinal salinity distribution and freshwater from the upstream reservoir in 2014.

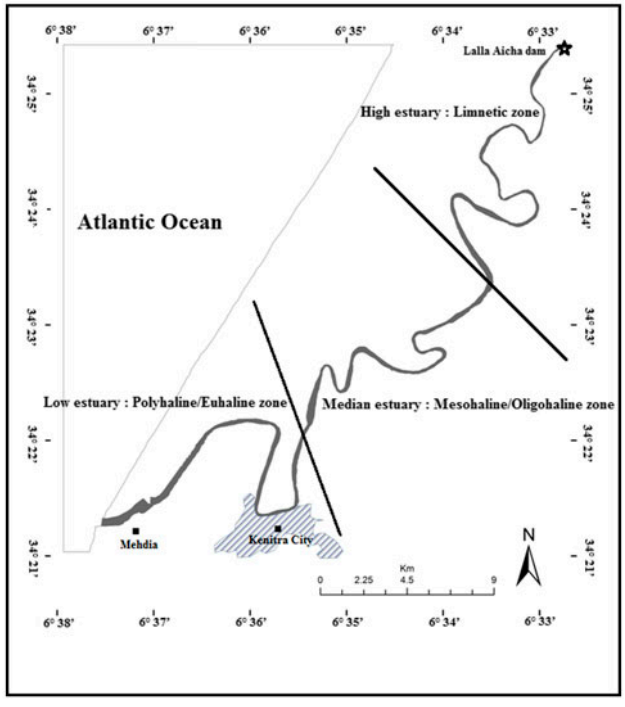

Fig. 5. Salinity zones in the Sebou river estuary.

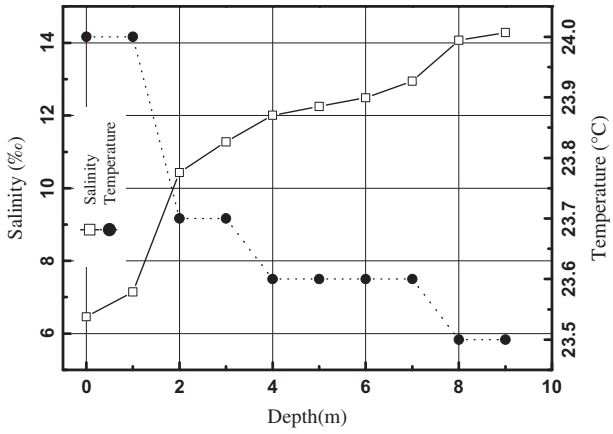

Fig. 6. Measured vertical salinity and temperature at the S3 station.

based on the one-dimensional transport equation (advection–dispersion equation) of a conservative constituent [11]:

$$\frac{\partial(AC)}{\partial t} + \frac{\partial(QC)}{\partial x} = \frac{\partial}{\partial x}\left[D.A\frac{\partial C}{\partial x}\right] \quad (9)$$

where C is the salinity concentration (‰), A is the cross-sectional area (m^2), Q is the river flow ($m^3\ s^{-1}$), and D is the longitudinal dispersion coefficient ($m^2\ s^{-1}$).

Velocity and water level appearing in the transport equation are calculated in the hydrodynamic module, which is linked to the water quality model.

The transport equation is solved using the Quickest-Ultimate numerical explicit scheme [11]. Inputs of the transport model are initial and boundary salinity

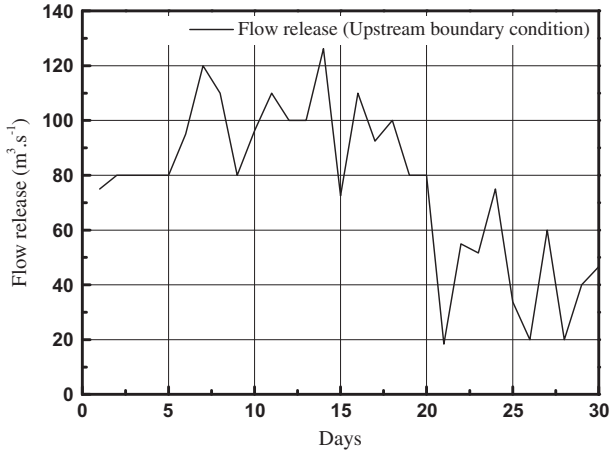

Fig. 7. Upstream boundary condition (at Lalla Aïcha dam), May 2014.

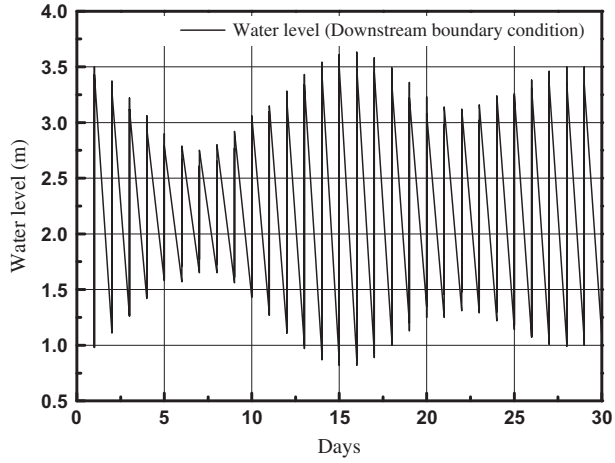

Fig. 8. Downstream boundary condition (at Mouth), May 2014.

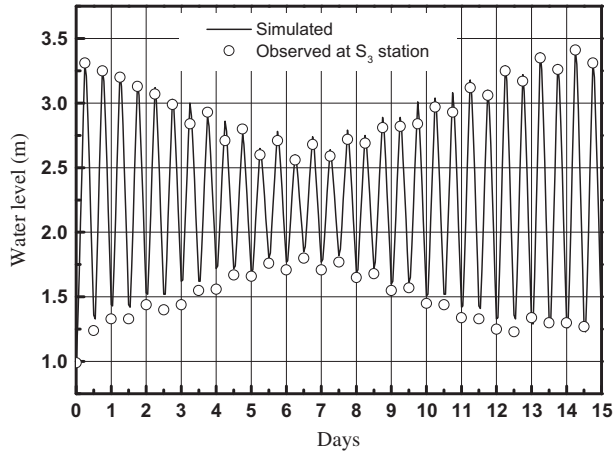

Fig. 9. Water level calibration at the S3 station: during 1 May 2014–15 May 2014.

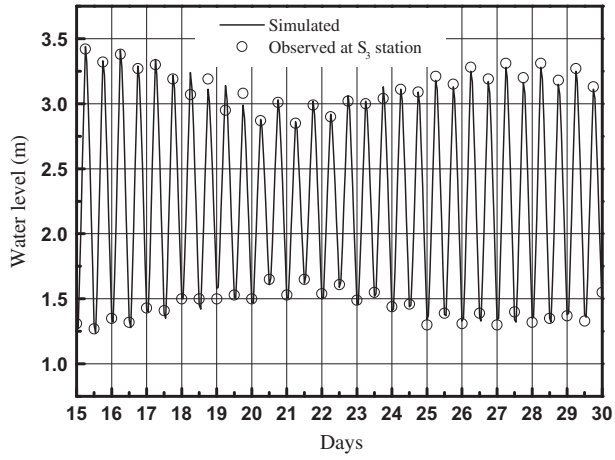

Fig. 10. Water level validation at the S3 station: during 15 May 2014–30 May 2014.

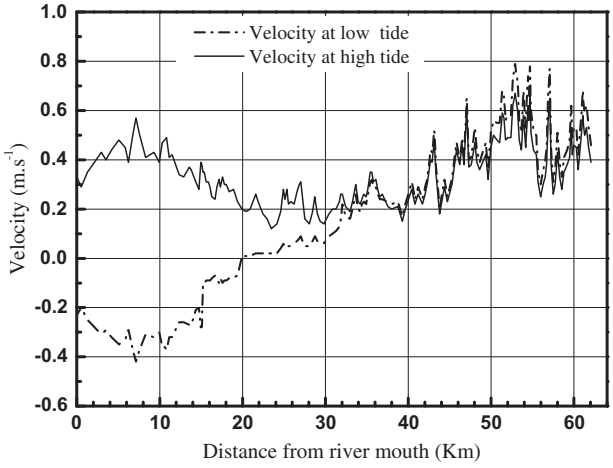

Fig. 11. Velocity profile at low tide and high tide, along the studied reach reproduced by the model.

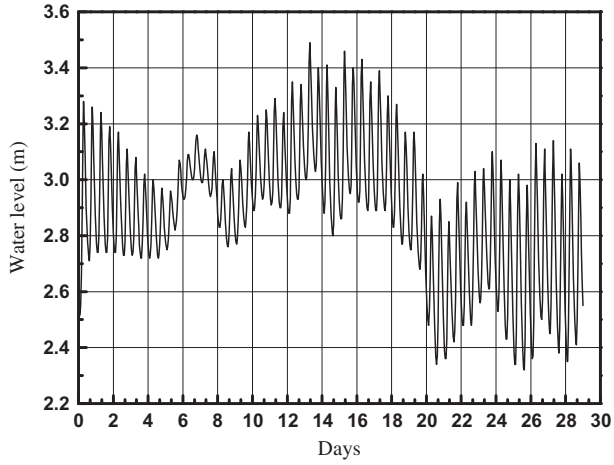

Fig. 12. Water level reproduced by the model at the S6 station.

concentrations and the dispersion coefficient (parameter D in Eq. (9)). Estimation of the dispersion coefficient equal to 50.48 $m^2 s^{-1}$ was calculated using Fischer formula [24].

3.2.2.1. Transport results. Simulated scenarios were defined considering the two influences on salinity intrusion which are river flow (releases from the Lalla Aïcha dam) and tidal situation (low or high tide).

Figs. 13–18 show the results of these simulations for three characteristic flows: 0 $m^3 s^{-1}$ (closed dam), 100 $m^3 s^{-1}$, 1,000 $m^3 s^{-1}$. This type of figures gives a isohaline charts (areas of equal salinity) for different situations (N.B. each legend is relative for each flow).

Figs. 13 and 14 show that when no flow is released from the Lalla Aïcha (upstream end), the level of salt in the reach is controlled by the movement of the tide.

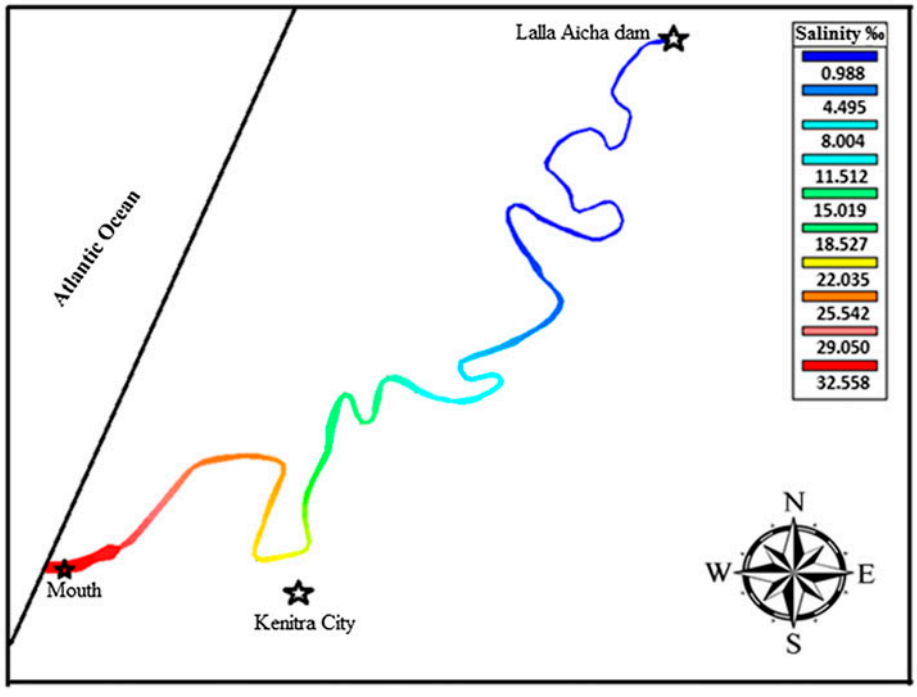

Fig. 13. Salinity evolution along the Sebou estuary at Low tide and freshwater from the upstream reservoir 0 $m^3 s^{-1}$.

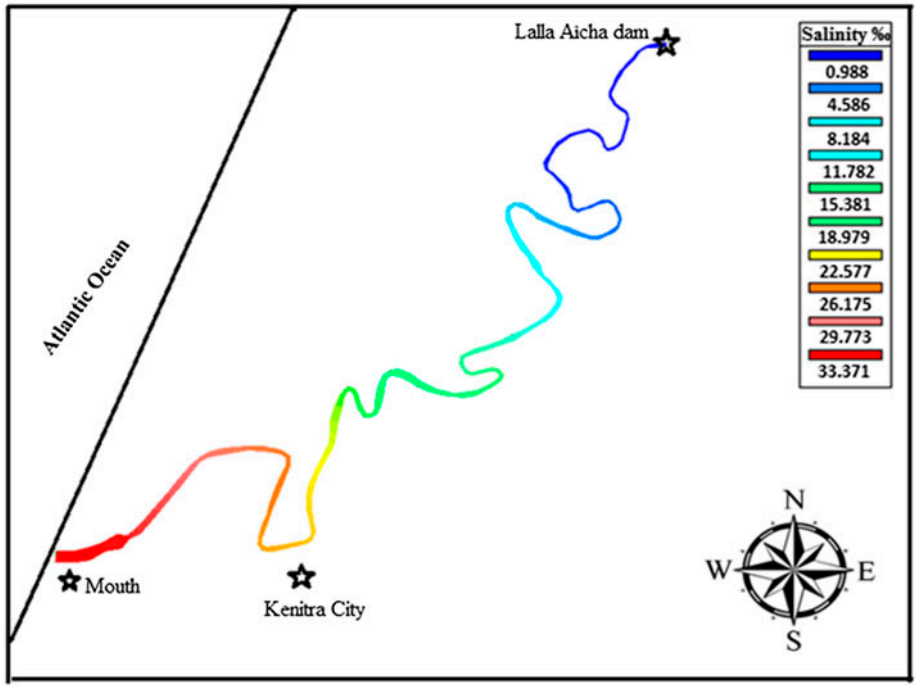

Fig. 14. Salinity evolution along the Sebou estuary at High tide and freshwater from the upstream reservoir 0 $m^3 s^{-1}$.

At high tide, excessive salinity is moved up to S6 station and varies between 8.18 and 11.78‰. At low tide, excessive salinity reached S5 station (8‰). An increase in the river fresh water flow to 100 $m^3 s^{-1}$ forces back the excessive salinity, which does not exceed S4 station, in low tide and high tide; this is

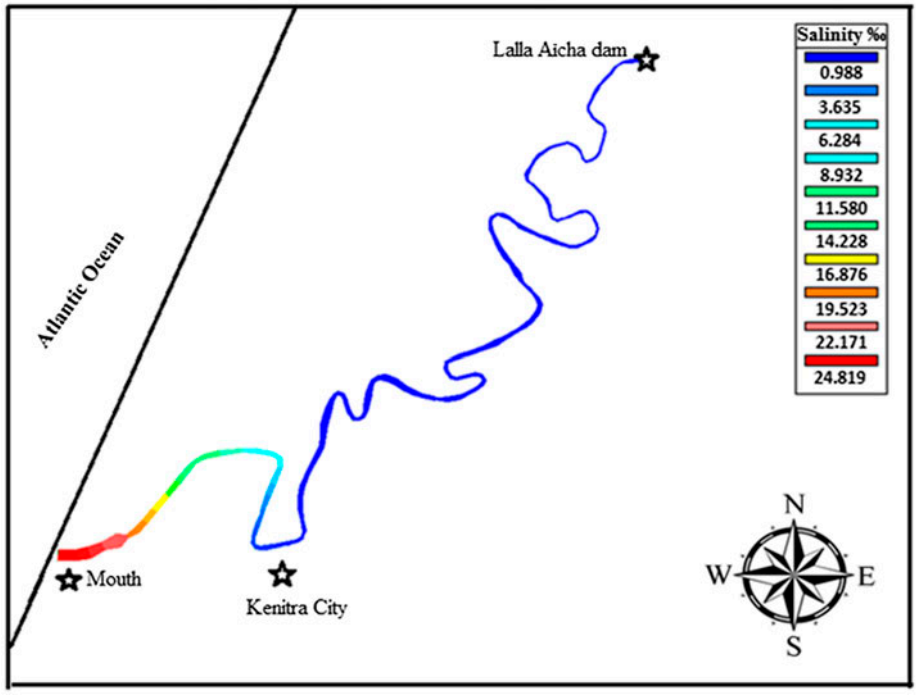

Fig. 15. Salinity evolution along the Sebou estuary at Low tide and freshwater from the upstream reservoir 100 $m^3 s^{-1}$.

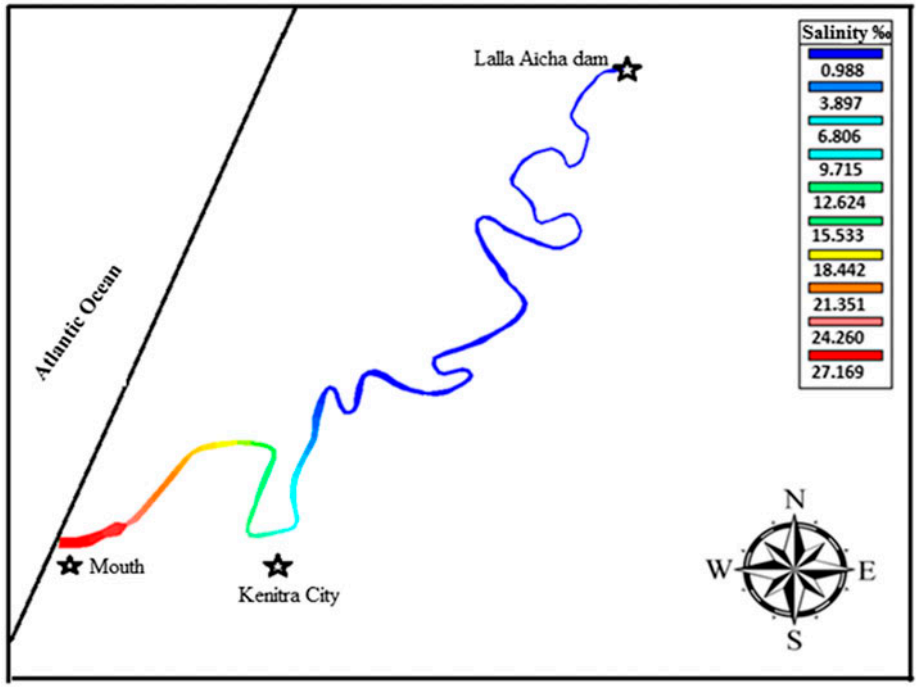

Fig. 16. Salinity evolution along the Sebou estuary at High tide and freshwater from the upstream reservoir 100 $m^3 s^{-1}$.

shown in Figs. 15 and 16. A river flow of 1,000 $m^3 s^{-1}$ stops the salinity in the vicinity of the river mouth and reduces its concentration, by dilution, to low values (7 and 12‰) (Figs. 17 and 18).

Hence, although the available data do not allow to simulate real events, the model outputs calculate salinity evolution that has the same evolutions as those observed in field measurements (Figs. 3 and 4).

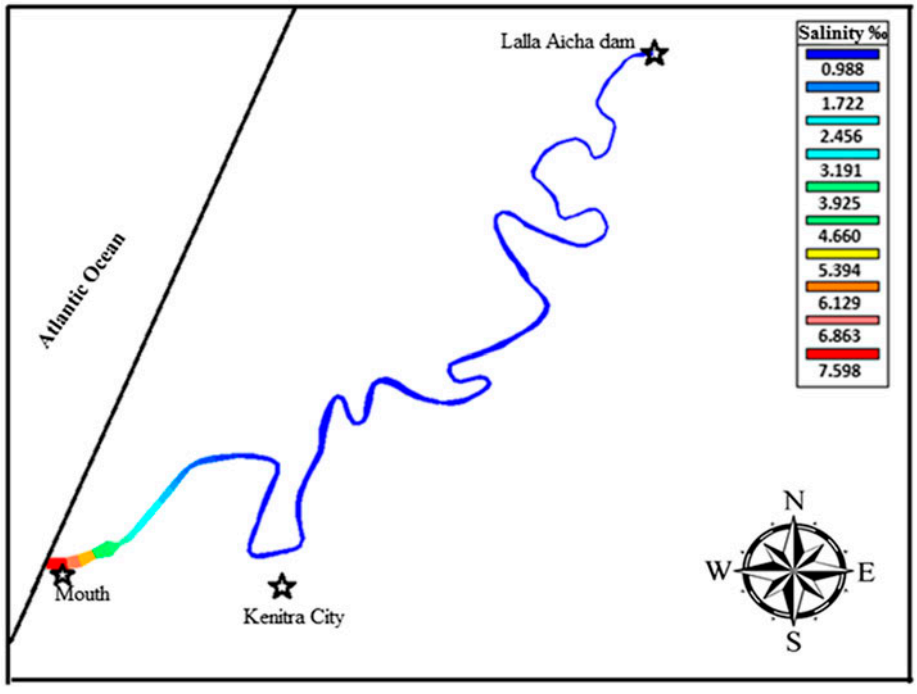

Fig. 17. Salinity evolution along the Sebou estuary at Low tide and freshwater from the upstream reservoir 1,000 $m^3 s^{-1}$.

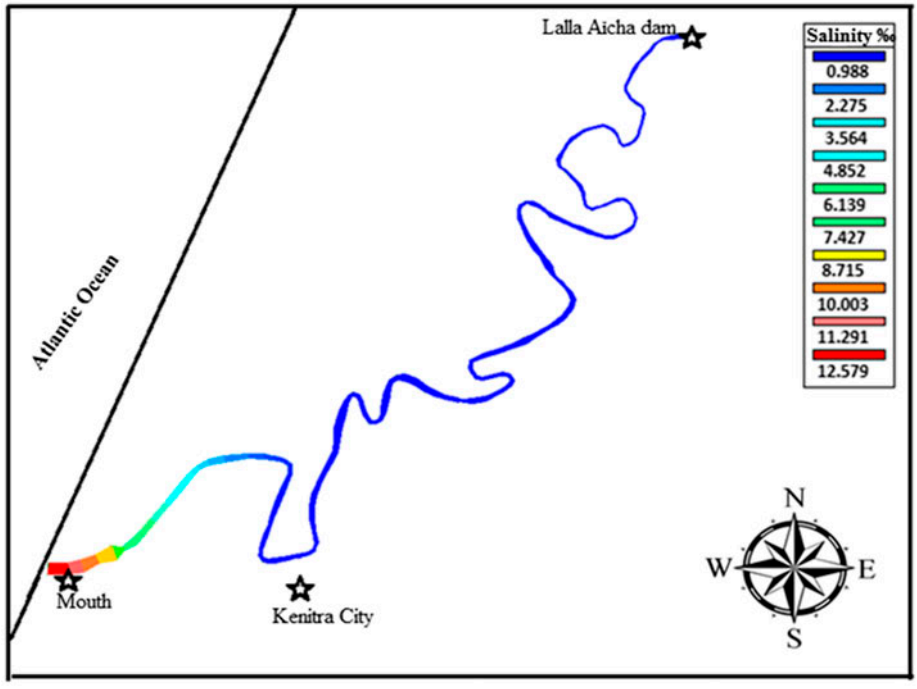

Fig. 18. Salinity evolution along the Sebou estuary at High tide and freshwater from the upstream reservoir 1,000 $m^3 s^{-1}$.

Summarizing, it can be seen that tide and river discharge are the two dominant drivers for the Sebou estuary. The salinity distribution confirmed the same pattern observed by other authors [7,8,12].

At this stage of the study, the model was used as a hypothesis verification tool, to analyze the consistency of measured, data and to understand the functioning of the estuary ecosystem.

Salinity simulations can be considered credible because the transport model is based on a hydrodynamic model which is calibrated and verified using field data.

Finally, the model used permits a rapid assessment of salt water intrusion in the Sebou estuary and can help to ensure the safety of water supply against excessive salinity. It calculates salinity adequately even at stations where we do not dispose of field measurements and can be considered as a tool for support decision-making.

4. Conclusion

The aim of this research is to understand the mechanisms of salt water intrusion in the Sebou river estuary and its dependence on hydrodynamic regime of the river. Field measurements were achieved for many situations of tidal cycle or river flow and revealed that tide and river discharge are the two dominant drivers for salinity distribution. Salinity measurements coupled with other basic data (river morphology, water stage, and boundary conditions) were used in a one-dimensional mathematical model. This model consists of a hydrodynamic module linked to a salt transport module. The hydrodynamic model was calibrated and validated, and gives the spatio-temporal evolution of velocity and depth. Salinity simulations provide longitudinal salt water distribution for many river situations, making the model as an early prediction and management tool. On other hand, the model outputs can serve as a starting point in many management projects relating to recreational, agricultural, commercial activities, and safe water supply.

Finally, our vertical salinity measurements show notable stratification essentially near the river mouth. However, the one-dimensional model used does not consider vertical salinity stratification in its mathematical formulation. Actual work emphasizes the study of the influence of this phenomenon on the predictions of one-dimensional model used.

Acknowledgment

The authors gratefully acknowledge the technicians at the Water Service of Kenitra town and the engineers of the National Agency of Ports for their availability and collaboration. They also thank Mr Othman Khabali for his contribution to the field measurements.

References

[1] A. Kettab, Water for all with quality and quantity: It is the concern of all! Desalin. Water Treat. 52 (2014) 1965–1966.

[2] D.W. Pritchard, What is an estuary? physical point of view, in: G.H. Lauff (Ed.), Estuaries, American Association for the Advancement of Science, Washington, DC, 1967, pp. 158–179.

[3] G.M.E. Perillo, Geomorphology and sedimentology of estuaries, Developments in Sedimentology 53, Elsevier Science, Amsterdam, (1995).

[4] M.D. Nazimuddin, A. Haque, M.D. Salequzzaman, A bio-physical relationship: biodiversity with salinity, J. Subtrop. Agric. Res. Dev. 8(3) (2010) 794–799.

[5] M. Igouzal, A. Maslousi, Water Modeling of the River Sebou Toward a Transdisciplinary Management Hydrocomplexity, IAHS-AISH Publication, 2010, pp. 106–107.

[6] M. Igouzal, A. Maslouhi, Elaboration of management tool of a reservoir dam on the Sebou river (Morocco) using an implicit hydraulic model, Hydraul. Res. J., 43 (2) (2005) 125–130.

[7] M. Combe, Hydrogeological maps of the Plain Gharb 1/100,000, Notes and Memoirs of the Geological Service of Morocco, No. 221 bis, Morocco, (1969), p. 39.

[8] S. El-Blidi, M. Fekhaoui, Hydrology and tidal dynamic in the Sebou estuary (Gharb, Morocco), Bull. Inst. Sci. Rabat, Sect. Life Sci. 25 (2003) 57–65.

[9] S. Haddout, A. Maslouhi M. Igouzal, Modélisation mathématique du régime d'écoulement de l'estuaire de la rivière Sebou (Maroc) (Mathematical modeling of the flow regime in the Sebou river estuary (Morocco)), National Water Information System Congress, NWIS 2014, December 2–4, Rabat.

[10] Z.G. Ji, Hydrodynamics and Water Quality: Modeling Rivers, Lakes, and Estuaries, John Wiley & Sons, Hoboken, NJ, 2008.

[11] G.W. Brunner, HEC-RAS river analysis system hydraulic reference manual (Version 4.1), US Army Corp of Engineers, Hydrologie Engineering Center (HEC), Davis California, USA, (2010).

[12] L. Mergaoui, M. Fekhaoui, D. Bouya, A. Gheït, A. Stambouli, Water quality and benthic macrofauna the estuarine environment of Morocco: The case of the Sebou estuary, Bull. Sci. Inst. Sect. Life Sci. 25 (2003) 67–75.

[13] Venice System. Symposium on the classification of brackish waters, Venice, April 8–14, 1958, Archives for Oceanography and Limnology 11 (Suppl.), 1958, pp. 1–248.

[14] A.T. Ippen, D.R.F. Harleman, One-dimensional Analysis of Salinity Intrusion in Estuaries. no 5 de Technical bulletin,United States. Army. Corps of Engineers. Committee on Tidal Hydraulics, Water ways Exp. Station, (1961).

[15] W.M. Cameron, D.W. Pritchard, Estuaries in the sea, in: M.N. Hill,(Eds.), vol. 2, John Wiley & Sons, New York, NY, 1963, pp. 306–324.

[16] A.M. Sanchez, Modélisation dans un estuaire à marée. Rôle du bouchon vaseux dans la tenue des sols sous marins (Modelling in a tidal estuary: Marine soils behaviour in the high turbidity zones), PhD thesis, Université de Nantes, Ecole Centrale de Nantes, (1992).

[17] V.T. Chow, Open-channel Hydraulics, McGraw-Hill International Editions, Civil Engineering Series, 1973.

[18] W. Cowan, Selecting Proper Friction Factors in River, McGraw-Hill International Editions, Civil Engineering Series, 1956.

[19] M. Billah, M.M. Rahman, A.S. Islam, G.T. Islam, S.K. Bala, S. Paul, M.A. Hasan, Impact of climate change on river flows in the southwest region of bangladesh, 5th International Conference on Water & Flood Management (ICWFM-2015).

[20] D.R. Legates, G.J. McCabe Jr., Evaluating the use of "goodness-of-fit" Measures in hydrologic and hydroclimatic model validation, Water Resour. Res. 35(1) (1999) 233–241.

[21] A. Stehr, P. Debels, F. Romero, H. Alcayaga, Hydrological modelling with SWAT under conditions of limited data availability: Evaluation of results from a Chilean case study, Hydrol. Sci. J. 53(3) (2008) 588–601.

[22] P. Zhang, J. Lu, L. Feng, X. Chen, L. Zhang, X. Xiao, H. Liu, Hydrodynamic and inundation modeling of China's largest freshwater lake aided by remote sensing data, Remote Sens. 7(4) (2015) 4858–4879.

[23] G.J. Doole, T. Ramilan, D.J. Pannell, Framework for evaluating management interventions for water-quality improvement across multiple agents, Environ. Modell. Software 26 (2011) 860–872.

[24] H.B. Fischer, Mixing in Inland and Coastal Waters, New York, NY: Academic Press, 1979, 483 p.